## A ADVERSARIAL DOMAIN ADAPTATION (ADA)

ADA aims to transfer prediction knowledge learned from a source domain with labeled data to a target domain without labels, by learning domain-invariant features. Let $D_\phi(\boldsymbol{x}) = q_\phi(y|\boldsymbol{x})$ be the domain discriminator. The conventional formulation of ADA is as following:

$$\begin{aligned} \max_{\boldsymbol{\phi}} \mathcal{L}_\phi &= \mathbb{E}_{\boldsymbol{x}=G_\theta(\boldsymbol{z}),\boldsymbol{z}\sim p(\boldsymbol{z}|y=1)} \left[\log D_\phi(\boldsymbol{x})\right] + \mathbb{E}_{\boldsymbol{x}=G_\theta(\boldsymbol{z}),\boldsymbol{z}\sim p(\boldsymbol{z}|y=0)} \left[\log(1 - D_\phi(\boldsymbol{x}))\right], \\ \max_{\boldsymbol{\theta}} \mathcal{L}_\theta &= \mathbb{E}_{\boldsymbol{x}=G_\theta(\boldsymbol{z}),\boldsymbol{z}\sim p(\boldsymbol{z}|y=1)} \left[\log(1 - D_\phi(\boldsymbol{x}))\right] + \mathbb{E}_{\boldsymbol{x}=G_\theta(\boldsymbol{z}),\boldsymbol{z}\sim p(\boldsymbol{z}|y=0)} \left[\log D_\phi(\boldsymbol{x})\right]. \end{aligned} \tag{18}$$

Further add the supervision objective of predicting label $t(\boldsymbol{z})$ of data $\boldsymbol{z}$ in the source domain, with a classifier $f_\omega(t|\boldsymbol{x})$ parameterized with $\boldsymbol{\pi}$:

$$\max_{\boldsymbol{\omega},\boldsymbol{\theta}} \mathcal{L}_{\omega,\theta} = \mathbb{E}_{\boldsymbol{z}\sim p(\boldsymbol{z}|y=1)} \left[\log f_\omega(t(\boldsymbol{z})|G_\theta(\boldsymbol{z}))\right]. \tag{19}$$

We then obtain the conventional formulation of adversarial domain adaptation used or similar in (Ganin et al., 2016; Purushotham et al., 2017).

## B PROOF OF LEMMA 1

*Proof.*

$$\begin{aligned} &\mathbb{E}_{p_\theta(\boldsymbol{x}|y)p(y)} \left[\log q^r(y|\boldsymbol{x})\right] = \\ &- \mathbb{E}_{p(y)} \left[\mathrm{KL}\left(p_\theta(\boldsymbol{x}|y) \| q^r(\boldsymbol{x}|y)\right) - \mathrm{KL}(p_\theta(\boldsymbol{x}|y) \| p_{\theta_0}(\boldsymbol{x}))\right], \end{aligned} \tag{20}$$

where

$$\begin{aligned} &\mathbb{E}_{p(y)} \left[\mathrm{KL}(p_\theta(\boldsymbol{x}|y) \| p_{\theta_0}(\boldsymbol{x}))\right] \\ &= p(y=0) \cdot \mathrm{KL}\left(p_\theta(\boldsymbol{x}|y=0) \| \frac{p_{\theta_0}(\boldsymbol{x}|y=0) + p_{\theta_0}(\boldsymbol{x}|y=1)}{2}\right) \\ &\quad + p(y=1) \cdot \mathrm{KL}\left(p_\theta(\boldsymbol{x}|y=1) \| \frac{p_{\theta_0}(\boldsymbol{x}|y=0) + p_{\theta_0}(\boldsymbol{x}|y=1)}{2}\right). \end{aligned} \tag{21}$$

Note that $p_\theta(\boldsymbol{x}|y=0) = p_{g_\theta}(\boldsymbol{x})$, and $p_\theta(\boldsymbol{x}|y=1) = p_{data}(\boldsymbol{x})$. Let $p_{M_\theta} = \frac{p_{g_\theta} + p_{data}}{2}$. Eq.(21) can be simplified as:

$$\mathbb{E}_{p(y)} \left[\mathrm{KL}(p_\theta(\boldsymbol{x}|y) \| p_{\theta_0}(\boldsymbol{x}))\right] = \frac{1}{2}\mathrm{KL}\left(p_{g_\theta} \| p_{M_{\theta_0}}\right) + \frac{1}{2}\mathrm{KL}\left(p_{data} \| p_{M_{\theta_0}}\right). \tag{22}$$

On the other hand,

$$\begin{aligned} \mathrm{JSD}(p_{g_\theta} \| p_{data}) &= \frac{1}{2}\mathbb{E}_{p_{g_\theta}}\left[\log \frac{p_{g_\theta}}{p_{M_\theta}}\right] + \frac{1}{2}\mathbb{E}_{p_{data}}\left[\log \frac{p_{data}}{p_{M_\theta}}\right] \\ &= \frac{1}{2}\mathbb{E}_{p_{g_\theta}}\left[\log \frac{p_{g_\theta}}{p_{M_{\theta_0}}}\right] + \frac{1}{2}\mathbb{E}_{p_{g_\theta}}\left[\log \frac{p_{M_{\theta_0}}}{p_{M_\theta}}\right] \\ &\quad + \frac{1}{2}\mathbb{E}_{p_{data}}\left[\log \frac{p_{data}}{p_{M_{\theta_0}}}\right] + \frac{1}{2}\mathbb{E}_{p_{data}}\left[\log \frac{p_{M_{\theta_0}}}{p_{M_\theta}}\right] \\ &= \frac{1}{2}\mathbb{E}_{p_{g_\theta}}\left[\log \frac{p_{g_\theta}}{p_{M_{\theta_0}}}\right] + \frac{1}{2}\mathbb{E}_{p_{data}}\left[\log \frac{p_{data}}{p_{M_{\theta_0}}}\right] + \mathbb{E}_{p_{M_\theta}}\left[\log \frac{p_{M_{\theta_0}}}{p_{M_\theta}}\right] \\ &= \frac{1}{2}\mathrm{KL}\left(p_{g_\theta} \| p_{M_{\theta_0}}\right) + \frac{1}{2}\mathrm{KL}\left(p_{data} \| p_{M_{\theta_0}}\right) - \mathrm{KL}\left(p_{M_\theta} \| p_{M_{\theta_0}}\right). \end{aligned} \tag{23}$$

Note that

$$\nabla_\theta \mathrm{KL}\left(p_{M_\theta} \| p_{M_{\theta_0}}\right)|_{\theta=\theta_0} = 0. \tag{24}$$

Taking derivatives of Eq.(22) w.r.t $\boldsymbol{\theta}$ at $\boldsymbol{\theta}_0$ we get

$$\begin{aligned} &\nabla_\theta \mathbb{E}_{p(y)} \left[\mathrm{KL}(p_\theta(\boldsymbol{x}|y) \| p_{\theta_0}(\boldsymbol{x}))\right]|_{\theta=\theta_0} \\ &= \nabla_\theta \left(\frac{1}{2}\mathrm{KL}\left(p_{g_\theta} \| p_{M_{\theta_0}}\right)|_{\theta=\theta_0} + \frac{1}{2}\mathrm{KL}\left(p_{data} \| p_{M_{\theta_0}}\right)\right)|_{\theta=\theta_0} \\ &= \nabla_\theta \mathrm{JSD}(p_{g_\theta} \| p_{data})|_{\theta=\theta_0}. \end{aligned} \tag{25}$$

Taking derivatives of the both sides of Eq.(20) at w.r.t $\boldsymbol{\theta}$ at $\boldsymbol{\theta}_0$ and plugging the last equation of Eq.(25), we obtain the desired results. □

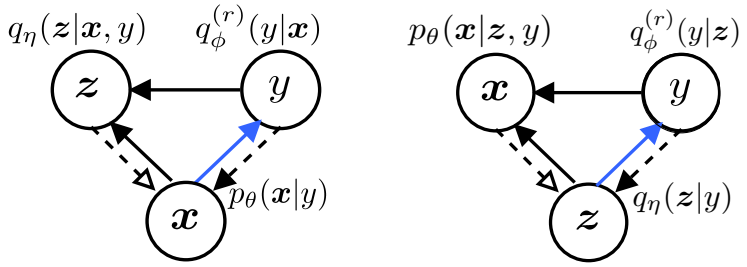


Figure 4: **Left:** Graphical model of InfoGAN. **Right:** Graphical model of Adversarial Autoencoder (AAE), which is obtained by swapping data $\boldsymbol{x}$ and code $\boldsymbol{z}$ in InfoGAN.

## C Proof of JSD Upper Bound in Lemma 1

We show that, in Lemma.1 (Eq.6), the JSD term is upper bounded by the KL term, i.e.,

$$\text{JSD}(p_\theta(\boldsymbol{x}|y=0)\|p_\theta(\boldsymbol{x}|y=1)) \leq \mathbb{E}_{p(y)}\left[\text{KL}(p_\theta(\boldsymbol{x}|y)\|q^r(\boldsymbol{x}|y))\right]. \tag{26}$$

*Proof.* From Eq.(20), we have

$$\mathbb{E}_{p(y)}\left[\text{KL}(p_\theta(\boldsymbol{x}|y)\|p_{\theta_0}(\boldsymbol{x}))\right] \leq \mathbb{E}_{p(y)}\left[\text{KL}\left(p_\theta(\boldsymbol{x}|y)\|q^r(\boldsymbol{x}|y)\right)\right]. \tag{27}$$

From Eq.(22) and Eq.(23), we have

$$\text{JSD}(p_\theta(\boldsymbol{x}|y=0)\|p_\theta(\boldsymbol{x}|y=1)) \leq \mathbb{E}_{p(y)}\left[\text{KL}(p_\theta(\boldsymbol{x}|y)\|p_{\theta_0}(\boldsymbol{x}))\right]. \tag{28}$$

Eq.(27) and Eq.(28) lead to Eq.(26). □

## D Schematic Graphical Models and AAE/PM/CycleGAN

**Adversarial Autoencoder (AAE)** (Makhzani et al., 2015) can be obtained by swapping code variable $\boldsymbol{z}$ and data variable $\boldsymbol{x}$ of InfoGAN in the graphical model, as shown in Figure 4. To see this, we directly write down the objectives represented by the graphical model in the right panel, and show they are precisely the original AAE objectives proposed in (Makhzani et al., 2015). We present detailed derivations, which also serve as an example for how one can translate a graphical model representation to the mathematical formulations. Readers can do similarly on the schematic graphical models of GANs, InfoGANs, VAEs, and many other relevant variants and write down the respective objectives conveniently.

We stick to the notational convention in the paper that parameter $\boldsymbol{\theta}$ is associated with the distribution over $\boldsymbol{x}$, parameter $\boldsymbol{\eta}$ with the distribution over $\boldsymbol{z}$, and parameter $\boldsymbol{\phi}$ with the distribution over $y$. Besides, we use $p$ to denote the distributions over $\boldsymbol{x}$, and $q$ the distributions over $\boldsymbol{z}$ and $y$.

From the graphical model, the inference process (dashed-line arrows) involves implicit distribution $q_\eta(\boldsymbol{z}|y)$ (where $\boldsymbol{x}$ is encapsulated). As in the formulations of GANs (Eq.4 in the paper) and VAEs (Eq.13 in the paper), $y=1$ indicates the real distribution we want to approximate and $y=0$ indicates the approximate distribution with parameters to learn. So we have

$$q_\eta(\boldsymbol{z}|y) = \begin{cases} q_\eta(\boldsymbol{z}|y=0) & y=0 \\ q(\boldsymbol{z}) & y=1, \end{cases} \tag{29}$$

where, as $\boldsymbol{z}$ is the hidden code, $q(\boldsymbol{z})$ is the prior distribution over $\boldsymbol{z}$[1], and the space of $\boldsymbol{x}$ is degenerated. Here $q_\eta(\boldsymbol{z}|y=0)$ is the implicit distribution such that

$$\boldsymbol{z} \sim q_\eta(\boldsymbol{z}|y=0) \quad \Longleftrightarrow \quad \boldsymbol{z} = E_\eta(\boldsymbol{x}),\ \ \boldsymbol{x} \sim p_{data}(\boldsymbol{x}), \tag{30}$$

[1]See section 6 of the paper for the detailed discussion on prior distributions of hidden variables and empirical distribution of visible variables

where $E_\eta(\boldsymbol{x})$ is a deterministic transformation parameterized with $\boldsymbol{\eta}$ that maps data $\boldsymbol{x}$ to code $\boldsymbol{z}$. Note that as $\boldsymbol{x}$ is a visible variable, the pre-fixed distribution of $\boldsymbol{x}$ is the empirical data distribution.

On the other hand, the generative process (solid-line arrows) involves $p_\theta(\boldsymbol{x}|\boldsymbol{z},y)q_\phi^{(r)}(y|\boldsymbol{z})$ (here $q^{(r)}$ means we will swap between $q^r$ and $q$). As the space of $\boldsymbol{x}$ is degenerated given $y=1$, thus $p_\theta(\boldsymbol{x}|\boldsymbol{z},y)$ is fixed without parameters to learn, and $\boldsymbol{\theta}$ is only associated to $y=0$.

With the above components, we maximize the log likelihood of the generative distributions $\log p_\theta(\boldsymbol{x}|\boldsymbol{z},y)q_\phi^{(r)}(y|\boldsymbol{z})$ conditioning on the variable $\boldsymbol{z}$ inferred by $q_\eta(\boldsymbol{z}|y)$. Adding the prior distributions, the objectives are then written as

$$\begin{aligned}&\max_{\boldsymbol{\phi}} \mathcal{L}_\phi = \mathbb{E}_{q_\eta(\boldsymbol{z}|y)p(y)}\left[\log p_\theta(\boldsymbol{x}|\boldsymbol{z},y)q_\phi(y|\boldsymbol{z})\right]\\ &\max_{\boldsymbol{\theta},\boldsymbol{\eta}} \mathcal{L}_{\theta,\eta} = \mathbb{E}_{q_\eta(\boldsymbol{z}|y)p(y)}\left[\log p_\theta(\boldsymbol{x}|\boldsymbol{z},y)q_\phi^r(y|\boldsymbol{z})\right].\end{aligned} \tag{31}$$

Again, the only difference between the objectives of $\boldsymbol{\phi}$ and $\{\boldsymbol{\theta},\boldsymbol{\eta}\}$ is swapping between $q_\phi(y|\boldsymbol{z})$ and its reverse $q_\phi^r(y|\boldsymbol{z})$.

To make it clearer that Eq.(31) is indeed the original AAE proposed in (Makhzani et al., 2015), we transform $\mathcal{L}_\phi$ as

$$\begin{aligned}\max_{\boldsymbol{\phi}} \mathcal{L}_\phi &= \mathbb{E}_{q_\eta(\boldsymbol{z}|y)p(y)}\left[\log q_\phi(y|\boldsymbol{z})\right]\\ &= \frac{1}{2}\mathbb{E}_{q_\eta(\boldsymbol{z}|y=0)}\left[\log q_\phi(y=0|\boldsymbol{z})\right] + \frac{1}{2}\mathbb{E}_{q_\eta(\boldsymbol{z}|y=1)}\left[\log q_\phi(y=1|\boldsymbol{z})\right]\\ &= \frac{1}{2}\mathbb{E}_{\boldsymbol{z}=E_\eta(\boldsymbol{x}),\boldsymbol{x}\sim p_{data}(\boldsymbol{x})}\left[\log q_\phi(y=0|\boldsymbol{z})\right] + \frac{1}{2}\mathbb{E}_{\boldsymbol{z}\sim q(\boldsymbol{z})}\left[\log q_\phi(y=1|\boldsymbol{z})\right].\end{aligned} \tag{32}$$

That is, the discriminator with parameters $\boldsymbol{\phi}$ is trained to maximize the accuracy of distinguishing the hidden code either sampled from the true prior $p(\boldsymbol{z})$ or inferred from observed data example $\boldsymbol{x}$. The objective $\mathcal{L}_{\theta,\eta}$ optimizes $\boldsymbol{\theta}$ and $\boldsymbol{\eta}$ to minimize the reconstruction loss of observed data $\boldsymbol{x}$ and at the same time to generate code $\boldsymbol{z}$ that fools the discriminator. We thus get the conventional view of the AAE model.

**Predictability Minimization (PM)** (Schmidhuber, 1992) is the early form of adversarial approach which aims at learning code $\boldsymbol{z}$ from data such that each unit of the code is hard to predict by the accompanying code predictor based on remaining code units. AAE closely resembles PM by seeing the discriminator as a special form of the code predictors.

**CycleGAN** (Zhu et al., 2017) is the model that learns to translate examples of one domain (e.g., images of horse) to another domain (e.g., images of zebra) and vice versa based on unpaired data. Let $\boldsymbol{x}$ and $\boldsymbol{z}$ be the variables of the two domains, then the objectives of AAE (Eq.31) is precisely the objectives that train the model to translate $\boldsymbol{x}$ into $\boldsymbol{z}$. The reversed translation is trained with the objectives of InfoGAN (Eq.9 in the paper), the symmetric counterpart of AAE.

## E Proof of Lemme 2

*Proof.* For the reconstruction term:

$$\begin{aligned}&\mathbb{E}_{p_{\theta_0}(\boldsymbol{x})}\left[\mathbb{E}_{q_\eta(\boldsymbol{z}|\boldsymbol{x},y)q_*^r(y|\boldsymbol{x})}\left[\log p_\theta(\boldsymbol{x}|\boldsymbol{z},y)\right]\right]\\ &= \frac{1}{2}\mathbb{E}_{p_{\theta_0}(\boldsymbol{x}|y=1)}\left[\mathbb{E}_{q_\eta(\boldsymbol{z}|\boldsymbol{x},y=0),y=0\sim q_*^r(y|\boldsymbol{x})}\left[\log p_\theta(\boldsymbol{x}|\boldsymbol{z},y=0)\right]\right]\\ &+ \frac{1}{2}\mathbb{E}_{p_{\theta_0}(\boldsymbol{x}|y=0)}\left[\mathbb{E}_{q_\eta(\boldsymbol{z}|\boldsymbol{x},y=1),y=1\sim q_*^r(y|\boldsymbol{x})}\left[\log p_\theta(\boldsymbol{x}|\boldsymbol{z},y=1)\right]\right]\\ &= \frac{1}{2}\mathbb{E}_{p_{data}(\boldsymbol{x})}\left[\mathbb{E}_{\tilde{q}_\eta(\boldsymbol{z}|\boldsymbol{x})}\left[\log \tilde{p}_\theta(\boldsymbol{x}|\boldsymbol{z})\right]\right] + const,\end{aligned} \tag{33}$$

where $y=0\sim q_*^r(y|\boldsymbol{x})$ means $q_*^r(y|\boldsymbol{x})$ predicts $y=0$ with probability 1. Note that both $q_\eta(\boldsymbol{z}|\boldsymbol{x},y=1)$ and $p_\theta(\boldsymbol{x}|\boldsymbol{z},y=1)$ are constant distributions without free parameters to learn; $q_\eta(\boldsymbol{z}|\boldsymbol{x},y=0)=\tilde{q}_\eta(\boldsymbol{z}|\boldsymbol{x})$, and $p_\theta(\boldsymbol{x}|\boldsymbol{z},y=0)=\tilde{p}_\theta(\boldsymbol{x}|\boldsymbol{z})$.

For the KL prior regularization term:

$$\begin{aligned}
&\mathbb{E}_{p_{\theta_0}(\boldsymbol{x})}\left[\mathrm{KL}(q_\eta(\boldsymbol{z}|\boldsymbol{x},y)q_*^r(y|\boldsymbol{x})\|p(\boldsymbol{z}|y)p(y))\right] \\
&= \mathbb{E}_{p_{\theta_0}(\boldsymbol{x})}\left[\int q_*^r(y|\boldsymbol{x})\mathrm{KL}\left(q_\eta(\boldsymbol{z}|\boldsymbol{x},y)\|p(\boldsymbol{z}|y)\right)dy + \mathrm{KL}\left(q_*^r(y|\boldsymbol{x})\|p(y)\right)\right] \\
&= \frac{1}{2}\mathbb{E}_{p_{\theta_0}(\boldsymbol{x}|y=1)}\left[\mathrm{KL}\left(q_\eta(\boldsymbol{z}|\boldsymbol{x},y=0)\|p(\boldsymbol{z}|y=0)\right) + const\right] + \frac{1}{2}\mathbb{E}_{p_{\theta_0}(\boldsymbol{x}|y=1)}\left[const\right] \\
&= \frac{1}{2}\mathbb{E}_{p_{data}(\boldsymbol{x})}\left[\mathrm{KL}(\tilde{q}_\eta(\boldsymbol{z}|\boldsymbol{x})\|\tilde{p}(\boldsymbol{z}))\right].
\end{aligned} \tag{34}$$

Combining Eq.(33) and Eq.(34) we recover the conventional VAE objective in Eq.(7) in the paper. □

## F VAE/GAN JOINT MODELS FOR MODE MISSING/COVERING

Previous works have explored combination of VAEs and GANs. This can be naturally motivated by the asymmetric behaviors of the KL divergences that the two algorithms aim to optimize respectively. Specifically, the VAE/GAN joint models (Larsen et al., 2015; Pu et al., 2017) that improve the sharpness of VAE generated images can be alternatively motivated by remedying the mode covering behavior of the KLD in VAEs. That is, the KLD tends to drive the generative model to cover all modes of the data distribution as well as regions with small values of $p_{data}$, resulting in blurred, implausible samples. Incorporation of GAN objectives alleviates the issue as the inverted KL enforces the generator to focus on meaningful data modes. From the other perspective, augmenting GANs with VAE objectives helps addressing the mode missing problem, which justifies the intuition of (Che et al., 2017a).

## G IMPORTANCE WEIGHTED GANS (IWGAN)

From Eq.(6) in the paper, we can view GANs as maximizing a lower bound of the "marginal log-likelihood" on $y$:

$$\begin{aligned}
\log q(y) &= \log \int p_\theta(\boldsymbol{x}|y)\frac{q^r(y|\boldsymbol{x})p_{\theta_0}(\boldsymbol{x})}{p_\theta(\boldsymbol{x}|y)}d\boldsymbol{x} \\
&\geq \int p_\theta(\boldsymbol{x}|y)\log\frac{q^r(y|\boldsymbol{x})p_{\theta_0}(\boldsymbol{x})}{p_\theta(\boldsymbol{x}|y)}d\boldsymbol{x} \\
&= -\mathrm{KL}(p_\theta(\boldsymbol{x}|y)\|q^r(\boldsymbol{x}|y)) + const.
\end{aligned} \tag{35}$$

We can apply the same importance weighting method as in IWAE (Burda et al., 2015) to derive a tighter bound.

$$\begin{aligned}
\log q(y) &= \log \mathbb{E}\left[\frac{1}{k}\sum_{i=1}^k \frac{q^r(y|\boldsymbol{x}_i)p_{\theta_0}(\boldsymbol{x}_i)}{p_\theta(\boldsymbol{x}_i|y)}\right] \\
&\geq \mathbb{E}\left[\log\frac{1}{k}\sum_{i=1}^k \frac{q^r(y|\boldsymbol{x}_i)p_{\theta_0}(\boldsymbol{x}_i)}{p_\theta(\boldsymbol{x}_i|y)}\right] \\
&= \mathbb{E}\left[\log\frac{1}{k}\sum_{i=1}^k w_i\right] \\
&:= \mathcal{L}_k(y)
\end{aligned} \tag{36}$$

where we have denoted $w_i = \frac{q^r(y|\boldsymbol{x}_i)p_{\theta_0}(\boldsymbol{x}_i)}{p_\theta(\boldsymbol{x}_i|y)}$, which is the unnormalized importance weight. We recover the lower bound of Eq.(35) when setting $k = 1$.

To maximize the importance weighted lower bound $\mathcal{L}_k(y)$, we take the derivative w.r.t $\boldsymbol{\theta}$ and apply the reparameterization trick on samples $\boldsymbol{x}$:

$$\begin{aligned}
\nabla_\theta\mathcal{L}_k(y) = \nabla_\theta\mathbb{E}_{\boldsymbol{x}_1,\ldots,\boldsymbol{x}_k}\left[\log\frac{1}{k}\sum_{i=1}^k w_i\right] &= \mathbb{E}_{\boldsymbol{z}_1,\ldots,\boldsymbol{z}_k}\left[\nabla_\theta\log\frac{1}{k}\sum_{i=1}^k w(y,\boldsymbol{x}(\boldsymbol{z}_i,\boldsymbol{\theta}))\right] \\
&= \mathbb{E}_{\boldsymbol{z}_1,\ldots,\boldsymbol{z}_k}\left[\sum_{i=1}^k \widetilde{w_i}\nabla_\theta\log w(y,\boldsymbol{x}(\boldsymbol{z}_i,\boldsymbol{\theta}))\right],
\end{aligned} \tag{37}$$

where $\widetilde{w_i} = w_i / \sum_{i=1}^k w_i$ are the normalized importance weights. We expand the weight at $\boldsymbol{\theta} = \boldsymbol{\theta}_0$

$$w_i|_{\theta=\theta_0} = \frac{q^r(y|\boldsymbol{x}_i)p_{\theta_0}(\boldsymbol{x}_i)}{p_\theta(\boldsymbol{x}_i|y)} = q^r(y|\boldsymbol{x}_i)\frac{\frac{1}{2}p_{\theta_0}(\boldsymbol{x}_i|y=0) + \frac{1}{2}p_{\theta_0}(\boldsymbol{x}_i|y=1)}{p_{\theta_0}(\boldsymbol{x}_i|y)}|_{\theta=\theta_0}. \tag{38}$$

The ratio of $p_{\theta_0}(\boldsymbol{x}_i|y=0)$ and $p_{\theta_0}(\boldsymbol{x}_i|y=1)$ is intractable. Using the Bayes' rule and approximating with the discriminator distribution, we have

$$\frac{p(\boldsymbol{x}|y=0)}{p(\boldsymbol{x}|y=1)} = \frac{p(y=0|\boldsymbol{x})p(y=1)}{p(y=1|\boldsymbol{x})p(y=0)} \approx \frac{q(y=0|\boldsymbol{x})}{q(y=1|\boldsymbol{x})}. \tag{39}$$

Plug Eq.(39) into the above we have

$$w_i|_{\theta=\theta_0} \approx \frac{q^r(y|\boldsymbol{x}_i)}{q(y|\boldsymbol{x}_i)}. \tag{40}$$

In Eq.(37), the derivative $\nabla_\theta \log w_i$ is

$$\nabla_\theta \log w(y, \boldsymbol{x}(\boldsymbol{z}_i, \boldsymbol{\theta})) = \nabla_\theta \log q^r(y|\boldsymbol{x}(\boldsymbol{z}_i, \boldsymbol{\theta})) + \nabla_\theta \log \frac{p_{\theta_0}(\boldsymbol{x}_i)}{p_\theta(\boldsymbol{x}_i|y)}. \tag{41}$$

The second term in the RHS of the equation is intractable as it involves evaluating the likelihood of implicit distributions. However, if we take $k = 1$, it can be shown that

$$\begin{aligned}
&- \mathbb{E}_{p(y)p(\boldsymbol{z}|y)}\left[\nabla_\theta \log \frac{p_{\theta_0}(\boldsymbol{x}(\boldsymbol{z}, \boldsymbol{\theta}))}{p_\theta(\boldsymbol{x}(\boldsymbol{z}, \boldsymbol{\theta})|y)}|_{\boldsymbol{\theta}=\boldsymbol{\theta}_0}\right] \\
&= -\nabla_\theta \frac{1}{2}\mathbb{E}_{p_\theta(\boldsymbol{x}|y=0)}\left[\frac{p_{\theta_0}(\boldsymbol{x})}{p_\theta(\boldsymbol{x}|y=0)}\right] + \frac{1}{2}\mathbb{E}_{p_\theta(\boldsymbol{x}|y=1)}\left[\frac{p_{\theta_0}(\boldsymbol{x})}{p_\theta(\boldsymbol{x}|y=1)}\right]|_{\theta=\theta_0} \\
&= \nabla_\theta \text{JSD}(p_{g_\theta}(\boldsymbol{x})\|p_{data}(\boldsymbol{x}))|_{\theta=\theta_0},
\end{aligned} \tag{42}$$

where the last equation is based on Eq.(23). That is, the second term in the RHS of Eq.(41) is (when $k = 1$) indeed the gradient of the JSD, which is subtracted away in the standard GANs as shown in Eq.(6) in the paper. We thus follow the standard GANs and also remove the second term even when $k > 1$. Therefore, the resulting update rule for the generator parameter $\boldsymbol{\theta}$ is

$$\nabla_\theta \mathcal{L}_k(y) = \mathbb{E}_{\boldsymbol{z}_1,\ldots,\boldsymbol{z}_k \sim p(\boldsymbol{z}|y)}\left[\sum_{i=1}^k \widetilde{w_i} \nabla_\theta \log q^r_{\phi_0}(y|\boldsymbol{x}(\boldsymbol{z}_i, \boldsymbol{\theta}))\right]. \tag{43}$$

## H ADVERSARY ACTIVATED VAEs (AAVAE)

In our formulation, VAEs include a degenerated adversarial discriminator which blocks out generated samples from contributing to model learning. We enable adaptive incorporation of fake samples by activating the adversarial mechanism. Again, derivations are straightforward by making symbolic analog to GANs.

We replace the perfect discriminator $q_*(y|\boldsymbol{x})$ in vanilla VAEs with the discriminator network $q_\phi(y|\boldsymbol{x})$ parameterized with $\boldsymbol{\phi}$ as in GANs, resulting in an adapted objective of Eq.(12) in the paper:

$$\max_{\boldsymbol{\theta},\boldsymbol{\eta}} \mathcal{L}^{\text{aavae}}_{\theta,\eta} = \mathbb{E}_{p_{\theta_0}(\boldsymbol{x})}\left[\mathbb{E}_{q_\eta(\boldsymbol{z}|\boldsymbol{x},y)q^r_\phi(y|\boldsymbol{x})}\left[\log p_\theta(\boldsymbol{x}|\boldsymbol{z}, y)\right] - \text{KL}(q_\eta(\boldsymbol{z}|\boldsymbol{x}, y)q^r_\phi(y|\boldsymbol{x})\|p(\boldsymbol{z}|y)p(y))\right]. \tag{44}$$

The form of Eq.(44) is precisely symmetric to the objective of InfoGAN in Eq.(9) with the additional KL prior regularization. Before analyzing the effect of adding the learnable discriminator, we first look at how the discriminator is learned. In analog to GANs in Eq.(3) and InfoGANs in Eq.(9), the objective of optimizing $\boldsymbol{\phi}$ is obtained by simply replacing the inverted distribution $q^r_\phi(y|\boldsymbol{x})$ with $q_\phi(y|\boldsymbol{x})$:

$$\max_{\boldsymbol{\phi}} \mathcal{L}^{\text{aavae}}_{\phi} = \mathbb{E}_{p_{\theta_0}(\boldsymbol{x})}\left[\mathbb{E}_{q_\eta(\boldsymbol{z}|\boldsymbol{x},y)q_\phi(y|\boldsymbol{x})}\left[\log p_\theta(\boldsymbol{x}|\boldsymbol{z}, y)\right] - \text{KL}(q_\eta(\boldsymbol{z}|\boldsymbol{x}, y)q_\phi(y|\boldsymbol{x})\|p(\boldsymbol{z}|y)p(y))\right]. \tag{45}$$

Intuitively, the discriminator is trained to distinguish between real and fake instances by predicting appropriate $y$ that selects the components of $q_\eta(\boldsymbol{z}|\boldsymbol{x}, y)$ and $p_\theta(\boldsymbol{x}|\boldsymbol{z}, y)$ to best reconstruct $\boldsymbol{x}$. The difficulty of Eq.(45) is that $p_\theta(\boldsymbol{x}|\boldsymbol{z}, y = 1) = p_{data}(\boldsymbol{x})$ is an implicit distribution which is intractable for likelihood evaluation. We thus use the alternative objective as in GANs to train a binary classifier:

$$\max_{\boldsymbol{\phi}} \mathcal{L}^{\text{aavae}}_{\phi} = \mathbb{E}_{p_\theta(\boldsymbol{x}|\boldsymbol{z},y)p(\boldsymbol{z}|y)p(y)}\left[\log q_\phi(y|\boldsymbol{x})\right]. \tag{46}$$

# I EXPERIMENTS

## I.1 IMPORTANCE WEIGHTED GANS

We extend both vanilla GANs and class-conditional GANs (CGAN) with the importance weighting method. The base GAN model is implemented with the DCGAN architecture and hyperparameter setting (Radford et al., 2015). We do not tune the hyperparameters for the importance weighted extensions. We use MNIST, SVHN, and CIFAR10 for evaluation. For vanilla GANs and its IW extension, we measure inception scores (Salimans et al., 2016) on the generated samples. We train deep residual networks provided in the tensorflow library as evaluation networks, which achieve inception scores of $9.09$, $6.55$, and $8.77$ on the test sets of MNIST, SVHN, and CIFAR10, respectively. For conditional GANs we evaluate the accuracy of conditional generation (Hu et al., 2017). That is, we generate samples given class labels, and then use the pre-trained classifier to predict class labels of the generated samples. The accuracy is calculated as the percentage of the predictions that match the conditional labels. The evaluation networks achieve accuracy of $0.990$ and $0.902$ on the test sets of MNIST and SVHN, respectively.

## I.2 ADVERSARY ACTIVATED VAES

We apply the adversary activating method on vanilla VAEs, class-conditional VAEs (CVAE), and semi-supervised VAEs (SVAE) (Kingma et al., 2014). We evaluate on the MNIST data. The generator networks have the same architecture as the generators in GANs in the above experiments, with sigmoid activation functions on the last layer to compute the means of Bernoulli distributions over pixels. The inference networks, discriminators, and the classifier in SVAE share the same architecture as the discriminators in the GAN experiments.

We evaluate the lower bound value on the test set, with varying number of real training examples. For each minibatch of real examples we generate equal number of fake samples for training. In the experiments we found it is generally helpful to smooth the discriminator distributions by setting the temperature of the output sigmoid function larger than 1. This basically encourages the use of fake data for learning. We select the best temperature from $\{1, 1.5, 3, 5\}$ through cross-validation. We do not tune other hyperparameters for the adversary activated extensions.

Table 4 reports the full results of SVAE and AA-SVAE, with the average classification accuracy and standard deviations over 5 runs.

| | 1% | 10% |
|---|---|---|
| SVAE | 0.9412±.0039 | 0.9768±.0009 |
| AASVAE | **0.9425±.0045** | **0.9797±.0010** |

Table 4: Classification accuracy of semi-supervised VAEs and the adversary activated extension on the MNIST test set, with varying size of real labeled training examples.